Automatic Control of Excitation Parameters for Switched-Reluctance Motor Drives

Yilmaz Sozer David A. Torrey Erkan Mese

Advanced Energy Conversion, LLC
31 Ontario Street
Cohoes, NY 12047, USA

Abstract

This paper presents a new approach to the automatic control of the turn-on angle used to excite the switched-reluctance motor (SRM). The control algorithm determines the turn-on angle that supports the most efficient operation of the motor drive system, and consists of two pieces. The first piece of the control technique monitors the position of the first peak of the phase current (θ_p) and seeks to align this position with the angle where the inductance begins to increase (θ_m). The second piece of the controller monitors the peak phase current and advances the turn-on angle if the commanded reference current cannot be produced by the controller. The first piece of the controller tends to be active below base speed of the SRM, where phase currents can be built easily by the inverter and θ_p is relatively independent of θ_m. The second piece of the controller is active above base speed, where the peak of the phase currents tends to naturally occur at θ_m regardless of the current amplitude. The two pieces of the controller naturally exchange responsibility as a result of a change in command or operating point. The motor, inverter and control system are modeled in Simulink to demonstrate the operation of the system. The control technique is then applied to an experimental SRM system. Experimental operation documents that the technique provides for efficient operation of the drive.

1 Introduction

The switched-reluctance motor (SRM) produces torque through excitation that is synchronized to rotor position. The simplest excitation strategy for the SRM is generally described by three excitation parameters: the turn-on angle $\theta_{\rm on}$, the turn-off angle $\theta_{\rm off}$, and the reference current $I_{\rm ref}$. A control algorithm would typically use the same excitation parameters for each phase, implemented with the spatial shift consistent with the symmetrically displaced phase structure. Control of the excitation angles results in either positive net torque for motoring, or negative net torque for generating. Basic operation of the SRM is given in [1, 2, 3] and the references cited therein.

Efficient operation of the SRM, or any motor drive, is always of importance. Inefficiency leads to larger size, increased weight, and increased energy consumption. In order to maximize SRM efficiency, we seek to maximize the ratio of the average torque to RMS phase current, $T_{\rm avg}/I_{ph\rm rms}$. This ratio captures our intended goal of providing the required mechanical output with the minimum electrical input. This approach is valid for both drive applications that are tolerant of SRM torque ripple and applications that require extremely smooth torque production, though smooth torque production may require current shaping that cannot be characterized by the single parameter $I_{\rm ref}$.

This paper presents an automatic excitation angle control algorithm that supports efficient operation of the SRM over its entire speed region. This approach is an alternative to the self-tuning approach to optimization of excitation parameters [4, 5] or an approach based on extensive look-up tables. The algorithm is given in Sec. 2. The operation of the algorithms is verified through simulation in Sec. 3. Section 4 provides operational verification on a 1 kW experimental SRM drive.

2 The Algorithm

The objectives of the algorithm are best explained through consideration of the linear inductance profile for the SRM shown in Fig. 1. The minimum inductance region is defined by the angular interval over which the rotor poles do not overlap the stator poles. The maximum inductance region is defined by the angular interval over which there is complete overlap between the stator and rotor poles. The regions of increasing and decreasing inductance correspond to varying overlap between the stator and rotor poles.

For operation as a motor, the SRM phase currents must be present in the phase winding as the inductance is increasing in the direction of rotation. For operation as a generator, the SRM phase currents must be present in the phase winding as the inductance is decreasing in the direction of rotation. The polarity of current is

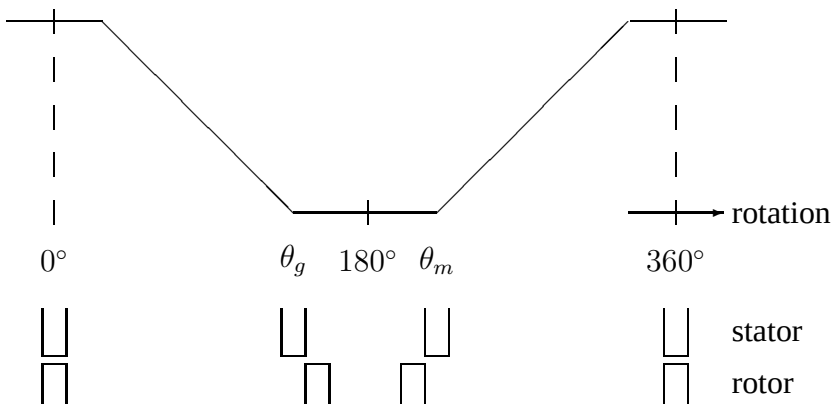

Figure 1: The linear inductance profile of the SRM showing θ_g and θ_m.

immaterial, so we assume that the phase currents are always positive.

If one were to examine the static torque curve for a typical SRM, it would be observed that the maximum torque for a given amount of current occurs as the rotor begins to move out of the minimum inductance position. This observation suggests that maximum torque per Ampere is produced upon leaving the minimum inductance position. Iron permeance causes torque production to fall off as overlap between the stator and rotor poles increases. In applications where average torque is of primary importance, it is important to make the most of the region near the unaligned position. Because it takes time to build the phase currents, we must anticipate the arrival of the torque production region. We must, therefore, turn on the phase windings before the angle marked θ_m in Fig. 1 so that the current is at $I_{\rm ref}$ when the rotor reaches θ_m.

We have modeled our experimental SRM drive to support simulation studies. The SRM magnetics have been modeled through finite element analysis to capture the relevant spatial and magnetic nonlinearities that must be considered for meaningful control design. For a speed of 1000 rpm, $I_{\rm ref} = 70$ A and conduction angle $\theta_{\rm cond} = \theta_{\rm off} - \theta_{\rm on} = 145^\circ$, Fig. 2 shows the motor power output versus the place where the peak current occurs as $\theta_{\rm on}$ is varied. For the SRM under consideration, $\theta_m = 225^\circ$ and $\theta_g = 135^\circ$ (electrical). As shown in Fig. 2, maximum power is produced when the first peak current occurs at θ_m.

The conventional approach to determining $\theta_{\rm on}$ is to work backward from θ_m:

$$\theta_{\rm on} = \theta_m - \frac{L_{\rm min}\, I_{\rm ref}\, \omega}{V_{\rm dc}} \quad , \tag{1}$$

where $L_{\rm min}$ is the minimum inductance, $V_{\rm dc}$ is the dc bus voltage, ω is the rotor speed, and $I_{\rm ref}$ is the reference current level. Equation 1 assumes the inductance is constant during the region $[\theta_g, \theta_m]$. The inductance can be a function of the phase current, rotor position and temperature. At low speed this method can give reasonable performance. For operation over a wide speed range Eq. (1) starts to break down as the phase back emf voltage becomes more prominent. It is desired to have closed loop control that provides the turn-on angle making first peak of the phase current at θ_m without the need of accurate (nonlinear) motor parameters and measurement of the dc bus voltage.

The proposed closed loop control algorithm continuously monitors the position of the first peak of the phase current (θ_p). The turn-on is advanced or retarded automatically according to the error between θ_p and θ_m. This piece of the controller successfully places θ_p at θ_m. Above base speed the peak current naturally tends to occur near θ_m. At these speeds $\theta_{\rm on}$ has little impact on θ_p but significant impact on the magnitude of the current at θ_p. This phenomena can be observed from Fig. 4. The SRM is simulated at 2500 rpm with three different turn-on angles. For each of the turn-on angles θ_p occurs approximately at the same place with different current magnitudes. To reflect this, the algorithm forces the peak phase current to match the commanded phase current. Feedforward control of $\theta_{\rm on}$ using Eq. (1) is used to speed convergence to the correct value of $\theta_{\rm on}$. The control of $\theta_{\rm on}$ is summarized in Fig. 3.

If the controller is in current regulation mode I_p occurs close to $I_{\rm ref}$ so the error between I_p and $I_{\rm ref}$ does not have any effect on the command for $\theta_{\rm on}$. Below base speed, the piece of the controller responsible for keeping θ_p at θ_m effectively works to achieve the control objective. At high speed if the controller is in voltage control mode θ_p naturally occurs at θ_m. The piece of the controller responsible for forcing I_p to track $I_{\rm ref}$ effectively works to advance the turn on angle to keep I_p close to $I_{\rm ref}$. If the reference current or the motor speed is reduced drive enters into current regulation mode and θ_p occurs before θ_m. The piece of the controller responsible for forcing $\theta_p = \theta_m$ becomes active and brings θ_p to θ_m by retarding $\theta_{\rm on}$.

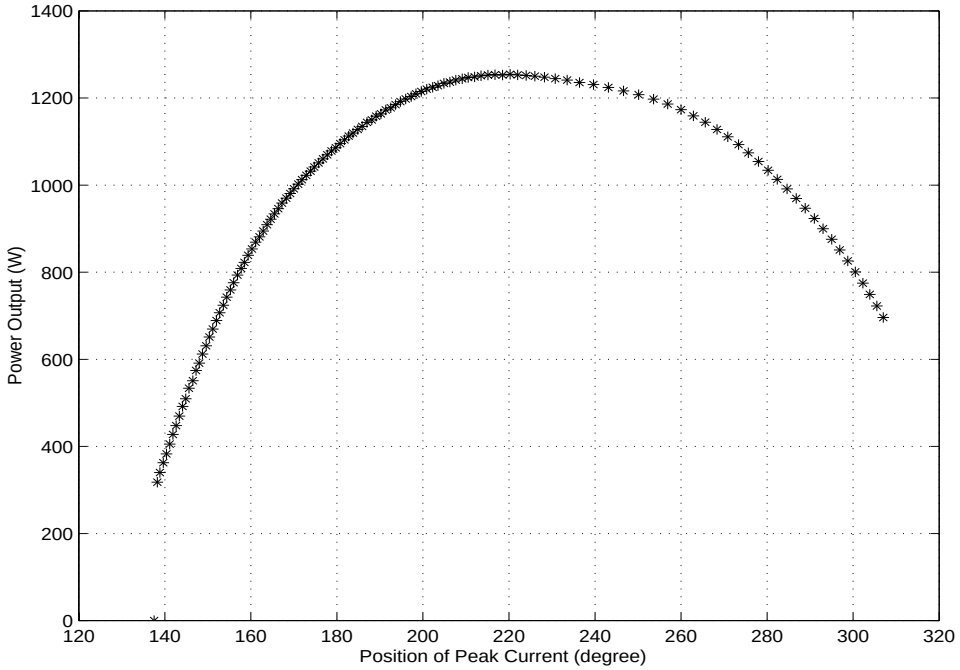

Figure 2: SRM power output as a function of the location where the current first reaches I_{ref}.

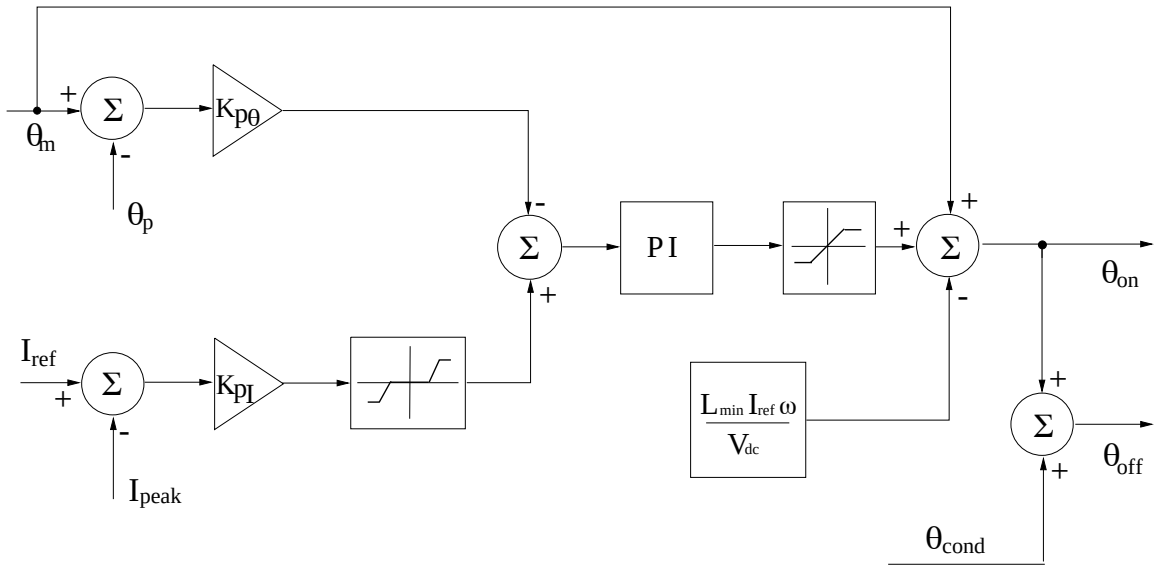

Figure 3: The algorithm used to automatically adjust the turn-on angle.

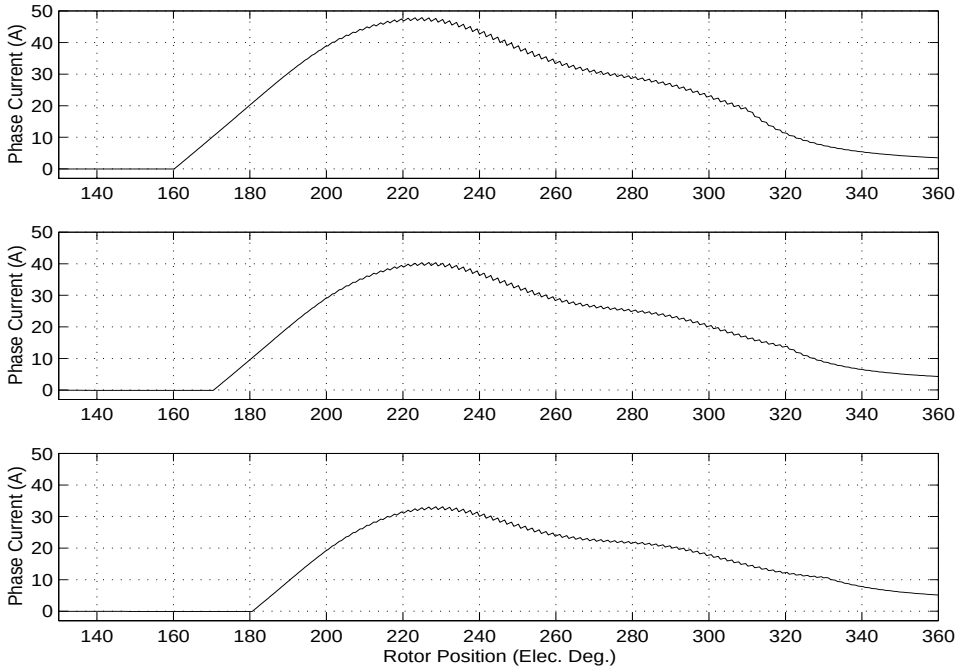

Figure 4: Phase currents at 2500 rpm with different turn-on angles.

3 Verification Through Simulation

The algorithm motivated in Sec. 2 was implemented in simulation to confirm proper operation before being experimentally implemented on the physical system. The SRM to which the simulation is applied is a 12/8 three-phase SRM designed for a 1 kW 42 V automotive application. The base speed of the SRM is 1000 rpm for an average torque of 10 Nm. The aligned phase inductance is 3.77 mH; the unaligned phase inductance is 0.32 mH. The SRM magnetics are modeled analytically based on finite element data as in [6].

Figure 5 shows the operation of the automatic controller for $\theta_{\rm on}$ for operation of the SRM at 1000 rpm with a commanded peak phase current of 70 A. The controller drives changes in $\theta_{\rm on}$ in order to force $\theta_p = \theta_m$ and $I_p = I_{\rm ref}$. At this speed the drive is able to produce the reference current easily and I_p is naturally close to $I_{\rm ref}$ without any control effort. $\theta_{\rm on}$ is heavily adjusted by the piece of the control that tries to force $\theta_p = \theta_m$. As we observe the motor torque production in Fig. 5 average torque production increases as θ_p approaches θ_m. The conduction angle $\theta_{\rm cond}$ is maintained at 145° (electrical) for all operating conditions.

Figure 6 shows the adjustment of the turn on angle at 2500 rpm. θ_p is close to θ_m throughout operation. The controller objective of keeping θ_p close to θ_m is naturally achieved. The other objective to produce the desired $I_{\rm ref}$ is achieved through the control.

Figure 7 shows the transient performance of the controller at 2500 rpm. The reference current is reduced from 50 A to 30 A at 0.05 s. The piece of the control responsible for forcing $I_p = I_{\rm ref}$ is incapable of sufficiently reducing the advance angle, so the current regulator becomes active. Excessive advance angle does not cause I_p to be greater than $I_{\rm ref}$ because the current regulator prevents the phase current from being greater than $I_{\rm ref}$. But because θ_p occurs earlier than θ_m, the piece of the controller that is responsible for forcing $\theta_p = \theta_m$ provides effort to reduce the advance angle to the correct value.

4 Experimental Results

The performance of the controller is experimentally verified with a 12/8 three-phase SRM designed for a 1kW 42V automotive application. The control algorithm of Sec. 2 is implemented using an Analog Devices ADMC401 digital signal processor. The SRM is coupled to an induction motor, which acts as a constant speed mechanical load through an adjustable speed drive. A shaft encoder provides direct, quadrature and index pulses to the quadrature encoder pulse unit of the DSP. A 42V battery is used throughout the tests to provide dc power to the inverter. Figure 8 shows a block diagram of the experimental setup for the tests.

Experimental tests are performed at a variety of operating points to show the effectiveness of the controller. Figure 9 shows the drive performance at 1000 rpm for a 20 A reference current with and without the closed loop angle controller. The analytically calculated advance angle does not find the advance angle accurately to make $\theta_p = \theta_m$. The closed loop angle controller on the other

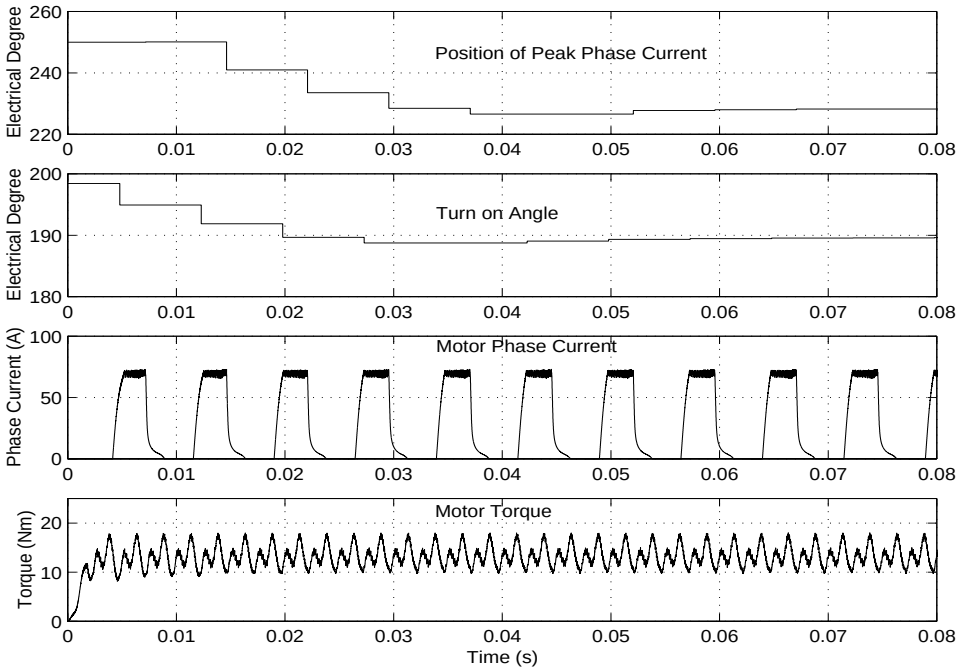

Figure 5: The automatic adjustment of $\theta_{\rm on}$ used to drive θ_p to θ_m at 1000 rpm for a 70 A reference current.

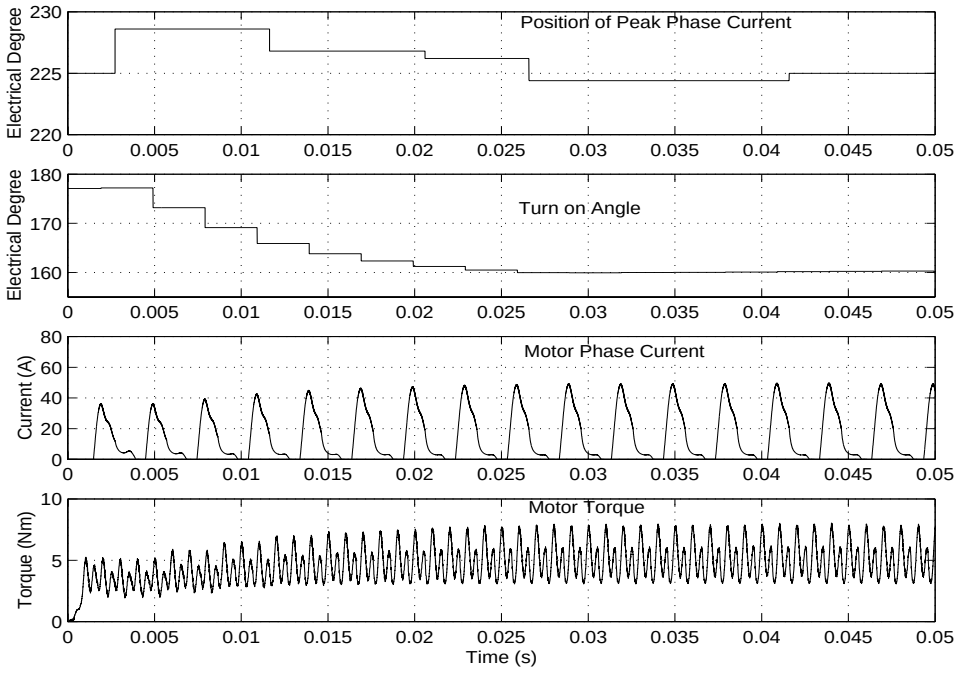

Figure 6: The automatic adjustment of $\theta_{\rm on}$ used to drive θ_p to θ_m at 2500 rpm for a 50 A reference current.

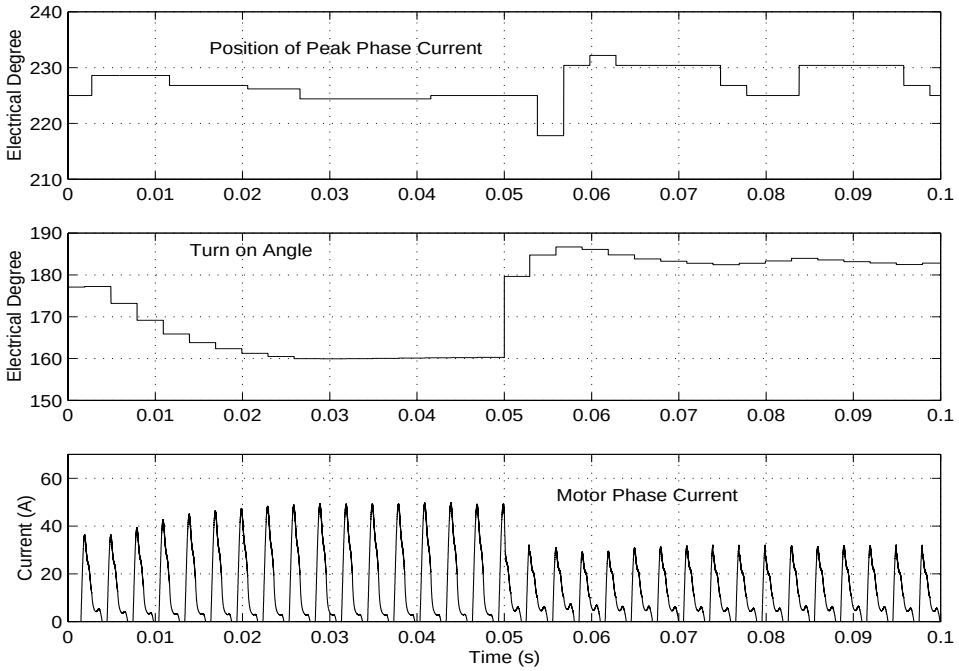

Figure 7: The automatic adjustment of $\theta_{\rm on}$ used to drive θ_p to θ_m at 2500 rpm when the reference current is reduced from 50 A to 30 A at 0.5 s.

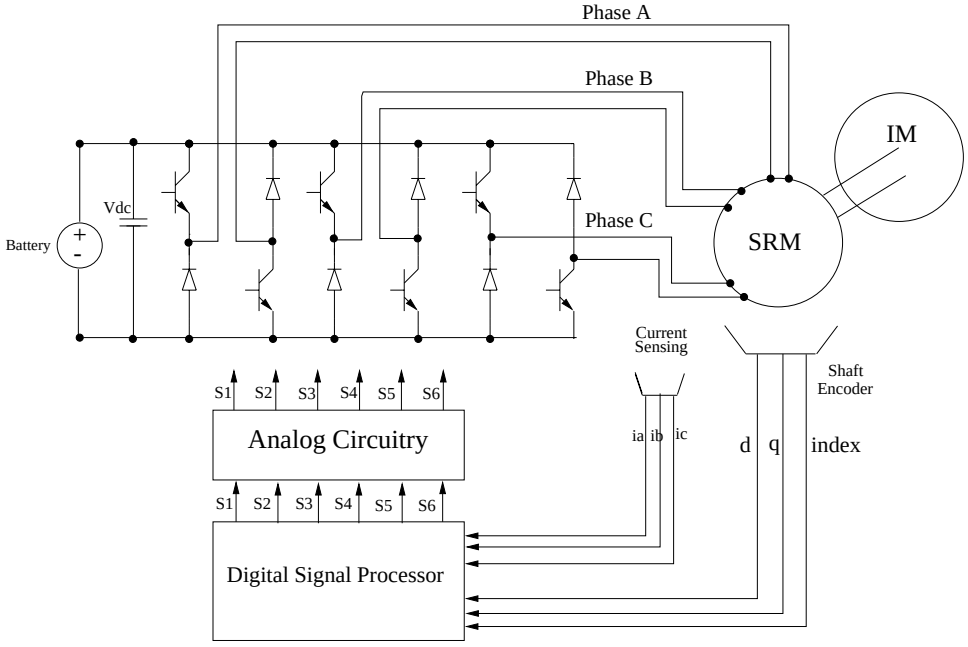

Figure 8: The block diagram of the experimental setup.

Figure 9: The performance of the experimental system with and without closed loop controller at 1000 rpm for a 20 A reference current.

hand produces the necessary advance angle to make $\theta_p = \theta_m$. Figure 10 shows a similar test for a 70 A reference current. Again performance of the drive is much better with the closed loop angle controller.

In Fig. 10, $\theta_{\rm on} = 168^\circ$ for closed loop operation and $\theta_{\rm on} = 195^\circ$ for open loop operation based only on the feedforward value of $\theta_{\rm on}$ predicted by Eq. 1. The corresponding system efficiencies are 59.1% and 58.8%, respectively. More importantly, the torques are 9.22 Nm and 8.04 Nm, respectively. The small drop in efficiency is not surprising given the broad efficiency optimum exhibited by the SRM. The electromechanical performance, however, drops substantially. In fact, the closed loop controller needs to command only 61.7 A of phase current to provide 8.04 Nm of torque, yielding an increased system efficiency of 62.7%.

Figure 11 shows the effectiveness of the controller at high speed. The closed loop controller effectively works to make both $\theta_p = \theta_m$ and $I_p = I_{\rm ref}$ at reference currents of 30 A and 50 A. The last graph in Fig. 11 shows the drive response without closed loop control. The drive without the closed loop control only produces 30 A in response to the reference of 50 A. It is worth noting that peak currents are occurring around the same rotor position irrespective of the turn on angle and peak current level. The 50 A peak current is produced with $\theta_{\rm on} = 137^\circ$; the 30 A peak current is produced with $\theta_{\rm on} = 169^\circ$. While the change in system efficiency for these two operating points is small (77.7% versus 77%), there is a substantial change in electromechanical performance. The torque for the 50 A reference is 3.22 Nm and the torque for the 30 A reference is 1.64 Nm. This again suggests that closed loop control of $\theta_{\rm on}$ substantially improves drive performance.

5 Summary

A new algorithm for the automatic control of $\theta_{\rm on}$ has been developed. The new approach provides for automatic turn-on angle adjustment without the need for motor parameters or self-tuning techniques. The algorithm monitors the peak phase current and where the peak current occurs. It places the position of the first peak of phase current at θ_m in order to maximize the torque per Ampere produced by the SRM. The controller also ensures that the peak phase current is equal to the reference current. The motor, inverter and control system are modelled in Simulink to demonstrate the operation of the system. The control technique was then applied to an experimental system. Both simulation and experimental results show that the new control technique provides efficient motor operation with easy implementation and without the need for motor parameters and load conditions.

References

[1] P. J. Lawrenson, et al., "Variable-speed switched reluctance motors," *IEE Proc.*, Vol. 127, pt. B, no. 4, pp. 253-265, 1980.

[2] T. J. E. Miller, *Switched Reluctance Motors and Their Control*, Oxford, 1993.

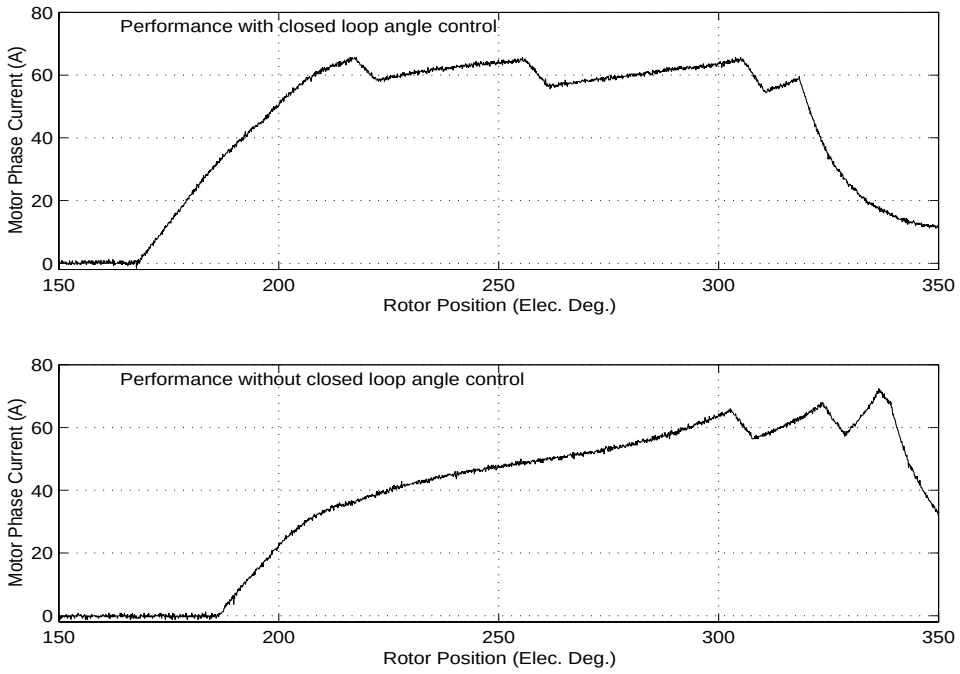

Figure 10: The performance of the experimental system with and without closed loop controller at 1000 rpm for a 70 A reference current.

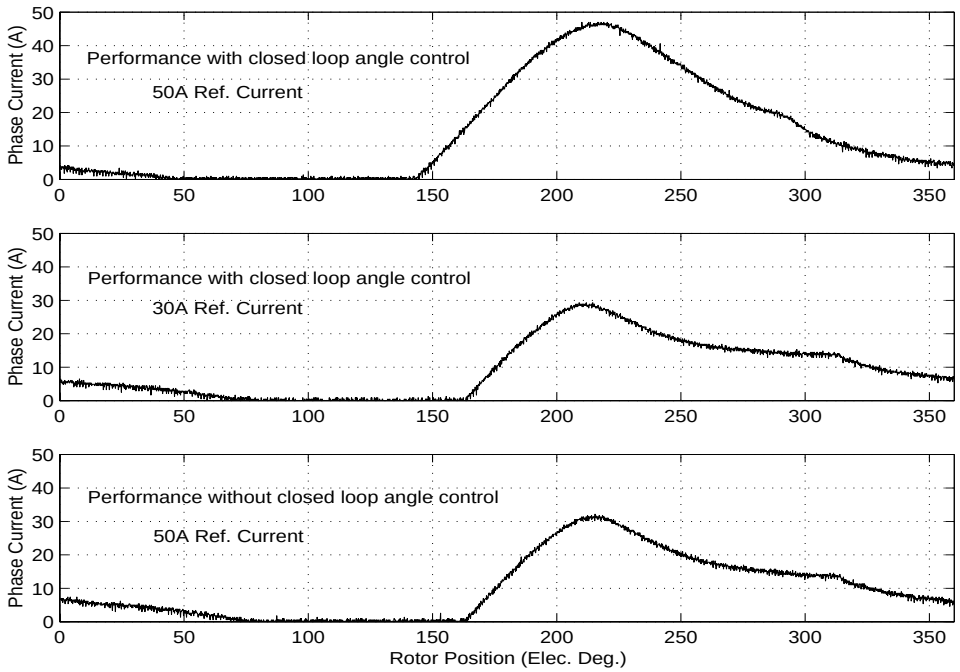

Figure 11: The performance of the experimental system with closed loop controller at 30 A and 50 A reference currents and without closed loop controller at 50 A reference current at 2500 rpm.

[3] R. Krishnan, *Switched Reluctance Motor Drives*, CRC Press, 2001.

[4] B. Fahimi, G. Suresh, J. P. Johnson, M. Ehsani, M. Arefeen and I. Panahi, "Self-tuning control of switched reluctance motors for optimized torque per Ampere at all operating points," *Proc. of the IEEE Applied Power Electronics Conf.*, pp. 778-783, 1998.

[5] K. Russa, I. Husain and M. Elbuluk, "A self-tuning controller for switched reluctance motors," *IEEE Trans. on Power Electronics*, Vol. 15, pp. 545-552, 2000.

[6] D. A. Torrey and J. H. Lang, "Modelling a nonlinear variable-reluctance motor drive," *IEE Proc.*, Vol. 137, pt. B, pp. 315-326, 1990.